ICSV13 - Vienna
The Thirteenth International Congress on Sound and Vibration
Vienna, Austria, July 2-6, 2006

# FREE VIBRATION ANALYSIS AND DYNAMIC BEHAVIOUR ON THE MULTILAYERED COMPOSITE PLATES FORMULATION

José P. Kai*[1]

[1]Department of Science and Technology, Angolan Jean-Piaget University
POB 81 Viana, Angola
jose.p.kai@exxonmobil.com

## Abstract

This paper deals with free vibrations analysis of multilayered plates. A set of dynamic equations for the plate are derived using a higher order shear deformation theory with a displacement field that includes five unknown parameters. Equivalent single layer theories were used. The employed theory is based on the same assumptions as the classical and first order shear deformation plate theories, except that the assumption on the straightness and normality of the transverse normal is relaxed. This generalized formulation covers symmetric as well as antisymmetric layer combinations. It is also a general case for classical, first order and previous higher order shear deformation theories. Finally, the governing equations are solved by Ritz method. Geometric factors, stacking pattern, transverse shear effect, in-plane strain and lamination stacking sequence will be compared to classical, first and higher order shear deformation theories.

## INTRODUCTION

A general formulation and numerical analysis are presented in this paper in order to study the free vibration of laminated composite plates. The equivalent single layer ESL laminate theories are applied. So that the stress or the displacement field is expressed as linear combination of both unknown functions and coordinate along the thickness. The theory is named $n^{th}$-order shear deformation theory if the in-plane displacements are expanded in terms of the thickness coordinate up to $n^{th}$ power.

Based on the literature(Deobald and Gibson 1988, Frederiksen 1995), it is clear the behaviour of composite plates subjected to free vibration was not well established, since none of approximate solutions obtained covered different types of theories, geometric factors, and different lamination stacking sequence of composite materials.

Eds.: J. Eberhardsteiner, H.A. Mang, H. Waubke

In addition, individual or combined effects such as shear deformation, rotary inertia and/or in-plane strains on the natural frequency of composite plates were not fully understood. In this paper, a general equivalent-layer formulation is employed to analyse the effect of the theories (Classical Laminated Plate Theory "CLPT",First-order and Higher-order Shear Deformation Theory "FSDT", "HSDT") on the natural frequencies of laminated composite plates. Moreover, the effect of fiber orientation on the natural frequency is investigated. In order to have better understanding of the dynamic behaviour of different plates with different parameters associated to the problem a dynamic analysis of composite plates is performed.

## FORMULATION OF THE PROBLEM

To model thick composites, the strain tensors as well as the strain components used in this paper are definied as reported by Kai and Viola, 2003.

### Higher-order shear deformation theory "HSDT"

***Case 1: Considering all effects "HSDT-1"*** The maximum total strain energy for higher-order theory is expressed by using the strain-displacement relations, constitutive equations and integrating over the thickness (Kai and Viola, 2003):

$$
\begin{aligned}
U_{max} = & \frac{1}{2}\int_{\Omega}[A_{11}(\varepsilon_{x0})^2 + 2B_{11}\varepsilon_{x0}\kappa_x + \Gamma_{11}(\kappa_x)^2 + 2A_{12}\varepsilon_{x0}\varepsilon_{y0} + 2B_{12}(\varepsilon_{y0}\kappa_y + \varepsilon_{y0}\kappa_x) \\
& + 2\Gamma_{12}\kappa_x\kappa_y + 2B_{22}\varepsilon_{y0}\kappa_y + A_{22}(\varepsilon_{y0})^2 + \Gamma_{22}(\kappa_y)^2 + 2A_{16}\varepsilon_{x0}\gamma_{xy0} + 2B_{16}(\gamma_{xy0}\kappa_x \\
& + \varepsilon_{x0}\kappa_{xy}) + 2\Gamma_{16}\kappa_x\kappa_{xy} + 2A_{26}\varepsilon_{y0}\gamma_{xy0} + 2B_{26}(\gamma_{xy0}\kappa_y + \varepsilon_{y0}\kappa_{xy}) + 2\Gamma_{26}\kappa_y\kappa_{xy} \\
& + \Gamma_{66}(\kappa_{xy})^2 + A_{66}(\gamma_{xy0})^2 + 2B_{66}\gamma_{xy0}\kappa_{xy}]dxdy \\
& + \frac{1}{2}\int_{\Omega}[A_{44}(\gamma_{xz0})^2 + 2A_{45}\gamma_{xz0}\gamma_{yz0} + A_{55}(\gamma_{yz0})^2]dxdy \qquad (1) \\
& + \frac{1}{2}\int_{\Omega}[2E_{11}\varepsilon_{x0}\kappa^s_x + 2F_{11}\kappa_x\kappa^s_x + H_{11}(\kappa^s_x)^2 + 2E_{12}(\varepsilon_{x0}\kappa^s_y + \varepsilon_{y0}\kappa^s_x) + 2F_{12}(\kappa_x\kappa^s_y \\
& + \kappa_y\kappa^s_x) + 2H_{12}\kappa^s_x\kappa^s_y + 2E_{22}\varepsilon_{y0}\kappa^s_y + 2F_{22}\kappa_y\kappa^s_y + H_{22}(\kappa^s_y)^2 + 2E_{16}(\kappa_{xy}\kappa^s_x + \varepsilon_{x0}\kappa^s_{xy}) \\
& + 2F_{16}(\kappa_x\kappa^s_{xy} + \kappa_{xy}\kappa^s_x) + 2H_{16}\kappa^s_x\kappa^s_{xy} + 2F_{26}(\kappa_y\kappa^s_{xy} + \kappa_{xy}\kappa^s_y) + 2H_{26}\kappa^s_y\kappa^s_{xy} \\
& + 2E_{26}(\kappa_{xy}\kappa^s_y + \varepsilon_{y0}\kappa^s_{xy}) + 2F_{66}\kappa_{xy}\kappa^s_{xy} + 4\Gamma_{45}\gamma_{xz0}\kappa^s_{yz} + 2F_{45}\kappa^s_{xz}\kappa^s_{yz} + 2\Gamma_{55}\gamma_{xy0}\kappa^s_{yz} \\
& + 2E_{66}\kappa_{xy}\kappa^s_{xy} + H_{66}(\kappa^s_{xy})^2 + 2\Gamma_{44}\gamma_{xz0}\kappa^s_{xz} + F_{44}(\gamma^s_{xz})^2 + F_{55}(\gamma^s_{yz})^2]dxdy,
\end{aligned}
$$

The maximum kinetic energy in the Ritz technique can be expressed in terms of displacement and slope functions and the specific mass of each layer $\rho_L$:

$$\begin{aligned}
\mathcal{T}_{max} &= \omega^2 \int_\Omega \sum_{L=1}^{NL} \rho_L \left[ \frac{z_L - z_{L-1}}{2}\left(u_0^2 + v_0^2 + w^2\right) + \frac{z_L^3 - z_{L-1}^3}{6}\left(\theta_x^2 + \theta_y^2\right) + \frac{z_L^2 - z_{L-1}^2}{2}\left(u_0\theta_x + v_0\theta_y\right)\right] dxdy \\
&+ \omega^2 \int_\Omega \sum_{L=1}^{NL} \rho_L \left\{ \frac{8\left(z_L^7 - z_{L-1}^7\right)}{63h^4}\left[\left(\frac{\partial w}{\partial x}\right)^2 + \left(\frac{\partial w}{\partial y}\right)^2\right] + \left[\frac{8\left(z_L^7 - z_{L-1}^7\right)}{63h^4} - \frac{4\left(z_L^5 - z_{L-1}^5\right)}{15h^2}\right]\left(\theta_x^2 + \theta_y^2\right) \right. \qquad (2) \\
&\left. + \left[\frac{16\left(z_L^7 - z_{L-1}^7\right)}{63h^4} - \frac{4\left(z_L^5 - z_{L-1}^5\right)}{15h^2}\right]\left(\theta_x \frac{\partial w}{\partial x} + \theta_y \frac{\partial w}{\partial y}\right) + \frac{z_{L-1}^4 - z_L^4}{3h^3}\left(u_0 \frac{\partial w}{\partial x} + v_0 \frac{\partial w}{\partial y} + u_0\theta_x + v_0\theta_y\right)\right\} dxdy.
\end{aligned}$$

The rigidities $A_{ij}, B_{ij}, \Gamma_{ij}, E_{ij}, F_{ij}, H_{ij}$ and deformations are defined as reported by Kai and Viola (2003).

***Case 2: Neglecting extension effects "HSDT-2"*** For this case the maximum kinetic energy and total strain energy for higher-order theory are obtained from Eqs (2) and (1) considering $u_0 = v_0 = \varepsilon_{x0} = \varepsilon_{y0} = 0$.

**First-order shear deformation theory "FSDT"**

***Case 3: Considering all effects "FSDT-1"*** The first integral in Eq. (2) corresponds to the maximum kinetic energy in the FSDT, whereas for the maximum total strain energy the third integral in Eq. (1) is neglected.

***Case 4: Neglecting extension effects "FSDT-2"*** The kinetic and the total strain energy in this case are obtained from case 3 deleting the terms associated with $u_0 = v_0 = \varepsilon_{x0} = \varepsilon_{y0} = 0$.

**Classical laminated plate theory "CLPT"**

In order to analyse the effect of transverse shear effect by the CLPT four cases have been considered:

***Case 5: Considering all effects "CLPT-1"*** The first integral in Eq. (2) corresponds to the maximum kinetic energy in the CLPT, which accounts the special relations $\theta_x = -\partial w/\partial x$ and $\theta_y = -\partial w/\partial y$ for this theory, whereas the maximum total strain energy considers only the first integral in Eq. (1).

***Case 6: Neglecting both shear deformation and rotary inertia "CLPT-2"*** For this case, considering the case 5, the shear and rotary inertia effects are neglected deleting the terms related with $u_0$ and $v_0$ in the first integral of Eq. (2).

***Case 7: Considering bending, shear deformation and rotary inertia effects "CLPT-3"*** For these cases, the maximum kinetic and total strain energies are obtained from case 5. This theory accounts zero the extension ($A_{ij}$) as well as the bending-extension coupling ($B_{ij}$) stiffnesses in the first integral of Eq.(1).

***Case 8: Neglecting both shear deformation and rotary inertia effects "CLPT-4"*** The last one case results from case 7. The shear and rotary inertia effects are neglected in the maximum kinetic energy.

## RITZ'S METHOD

In the Ritz technique, the assumed solutions are in the form of a finite linear combination of unknown coefficients with appropriate chosen functions. Each displacement function is represented by a finite set of functions.

The Ritz technique is applied in the usual manner, that is the functional $\mathcal{L}=U_{max}-\mathcal{T}_{max}$ is minimized with respect to the unknown coefficient. So that a set of simultaneous linear homogeneous equations can be written as an eigenvalue problem

$$\mathbf{K}\mathbf{v}_i - \lambda_i \mathbf{M}\mathbf{v}_i = \mathbf{0} \tag{3}$$

where **K** and **M** are stiffness and mass matrices, respectively, $\mathbf{v}_i$ is the eigenvector containing the unknown parameters corresponding to the eigenvalue $\lambda_i$ , which is related to the i'$^{th}$ eigenfrequency $\omega_i$ by $\lambda_i = \omega_i^2$.

## NUMERICAL RESULTS AND DISCUSSION

In this work the layers have equal thickness and the material properties in each layer of laminates are given as follows: $E_1/E_2 = E_1/E_3 = 20$, $E_2/G_{12} = E_2/G_{13} = 2$, $E_2/G_{23} = 3$, $\nu_{12} = \nu_{13} = 0.25$ and $\nu_{23} = 0.5$ i.e., the material is transversely isotropic.

Tab. 1 gives the first 10 nondimensional frequencies for three-layer [θ, -θ, θ] angle-ply rectangular plates of moderate thickness a/h=30. It is observed that by increasing the θ angle the first three frequencies are increased, thereby obtaining their maximum at θ=45°. The fundamental frequency increases by almost 50% by changing the angle from θ=0° to θ=45°.

Fig. 1 shows the fundamental frequency parameter for a cross-ply ([0°,90°,90°,0°], [90°,0°,0°,90°] and [90°,0°,90°,0°]) rectangular plates of various length-to-thickness ratios, respectively. The disagreement between the results obtained by the eight models is significant only for very thick plates. For decreasing thickness the frequencies converge monotonically from below. For symmetric plates, $B_{ij}=E_{ij}=0$ for i,j=1,2,6 thus , there is no bending-extension coupling stiffness (HDST-

1=HDST-2, FDST-1=FDST-2, CPLT-1=CPLT-3 and CPLT-2=CPLT-4). The transverse shear deformation effect on the plate natural frequencies for thin to moderately thick plates is also illustrated by Fig. 5. This Figure shows the difference of the frequencies for the different theories.

It can be seen that frequencies calculated according to HSDT theory are in most cases slightly lower than those from FSDT theory even though some frequencies for the orthotropic plate and the laminates are higher. The agreement between the two models for a moderately thick plate is good, both having the same number of d.o.f., despite the fact that the total strain energy for FSDT model comprises only 46 different terms, whereas for HSDT comprises 76 different terms (Kai and Viola, 2003). Hence, for moderately thick plates, model FSDT seems to provide an appropriate compromise between accuracy and computationally efficiency.

From Fig. 1 it can be seen that neglecting the transverse shear effect as for CLPT-4 and CLPT-2 theories frequencies are generally underestimated when compared to the consistent theory of type HSDT. Therefore, in the case of a very thick cross-ply plate the similar holds and some frequencies calculated with theory FSDT are slightly higher than those from theory HSDT. To this may be added the fact that the correspondence between the mode shapes of the two theories is less distinct for very thick plates.

It is worth noting that when reducing the HSDT theory to the CLPT theory two types of error are made. When bending-extension coupling and degree of freedom are reduced in the approximation, increased frequencies are observed. For the isotropic plate, the error is totally dominated by the neglected transverse normal effect and therefore the frequencies of theory HSDT may be lower than those of theory CLPT (Kai and Viola, 2003).

As was further expected, the CLPT yields always considerably higher flexural vibration frequencies with respect to the others theories. The inclusion of the rotary inertia terms (CLPT-2 and CPLT-4) improves the performance of the classical plate theory, especially when dealing with higher vibration modes, but it still yields considerably inaccurate results, as shown in Tab. 1.

As can be noticed, including shear deformation (CLPT-1 and CLPT-3) had significantly affected the natural frequency values, contrary to that when including rotary inertia (CLPT-2 and CLPT-4). Moreover, it should be indicated that the percentage change in the nondimensional fundamental frequencies due to the inclusion of shear deformation is dependent on the span-to-depth ratio. The results showed less effect of including shear deformations at higher span depth ratios, and at a lower mode number. As was expected, including both shear deformation and bending-extension coupling has affected more significantly the natural frequency values, principally for not symmetric plates (see Fig. 5).

Fig. 5 shows the effect of span-to-depth ratio (a/h) on the fundamental frequency of a rectangular cross-ply laminated orthotropic plate for cases from 1 to 8. At higher span-to-depth ratios greater than 30, the influence of including shear deformation on nondimensional frequencies is minor, although values remain smaller than those obtained for cases 6 (CLPT-2) and 8 (CLPT-4).

The obtained results show, as expected, that natural frequencies are higher for the angle-ply conditions than those for the cross-ply conditions. This is attributed to the stiffness, which is the highest in angle-ply plates and the lowest in cross-ply ones. The above results showed that the effect of shear deformation on an angle-ply plate is more than that on a cross-ply: the effective length between the neutral surface and the fiber component is increased.

As the aspect ratio increased, the nondimensional fundamental frequency increased. The results of Fig. 5 suggest that when shear and rotary inertia deformations are included, the rate of change of natural frequency to aspect ratio decreases. Moreover, it is clear that natural frequency is increased when adopting a laminae sequence in the manner [θ, 0°, 0°, θ], rather than ([0°, θ, θ, 0°], because the distance between the neutral surface and the fiber components is increased. This result does not appear in Fig. 6, where the cross-ply plate behaviour is shown.

It should be noted that the most interesting feature of the results shown in Figs 1-4 is the bending-extension coupling effect due to lamination, which tends to lower the fundamental frequency parameter. This coupling has its strongest effect on the frequency of a two-layered laminate, but it dies out very rapidly with increasing numbers of considered layers. In this respect, the multi-layered laminates $[\theta, -\theta]_5$ and $[\theta, -\theta]_{10}$ behave like essentially orthotropic plates, in which this lamination coupling effect does not practically exist. This is precisely the reason that makes sensibly identical all the corresponding results shown for $[\theta, -\theta]_5$ and $[\theta, -\theta]_{10}$ laminates.

On the other hand, it is very interesting to observe that the effect of coupling is very moderate on fundamental frequency of square plates. This effect becomes pronounced only on the fundamental frequency of relatively low values of lamination angle in rectangular plates ($15° \leq \theta \leq 30$) as shown in Figs 3 and 4. This can be attributed to the free edges and the cylindrical effect of the rectangular plates considered in this paper. For high values of the lamination angle ($75° \leq \theta \leq 90°$), the corresponding mode shape of [θ,-θ] and $[\theta, -\theta]_5$ laminates still appear to be identical and, despite the presence of the extension-bending coupling effect, they appear to be very similar even for θ=45° and θ=60°. It is only for θ=15° that the strong presence of the extension-bending coupling due to lamination makes the mode shape of the [15°,-15°] laminate differ considerably from that of the $[15°,-15°]_5$ one. All these effects are more evident for a rectangular laminate plate.

## CONCLUSIONS

Based on the results obtained before from eight different plate theories for completely free laminated plates, the following conclusions can be drawn:

a) The results from case 5 (CLPT-1) and 7 (CLPT-3) were proved to be better that those of the case 6 (CLPT-2) and 8 (CLPT-4) but were still considerably inferior than those based on the HSDT (Case 1 and 2).
b) Bending-extension coupling terms have a minor influence on the values of natural frequency on the CLPT than on the HSDT.

c) The effect of including transverse shear deformation is greater for angle-ply plates than for a cross-ply ones.
d) Fiber orientation θ has a great effect on the determination of natural frequencies of angle-ply composite plates. For a square plate, maximum fundamental frequency is obtained when fibers were oriented at an angle of 45°, while for rectangular plate the fundamental frequency depends of the (a/b) ratio.
e) It was observed that the bending-extension coupling effect due to lamination is very moderate on the fundamental frequencies of square plates while, for rectangular plates, it becomes pronounced on the fundamental frequencies of relatively less values of the lamination angle. This was attributed to the free edges and the cylindrical effect for the rectangular plate. The coupling effect appeared always to be more pronounced, regardless of the value of the lamination angle.

## REFERENCES

L.R.Deobald, R.F. Gibson, "Determination of elastic constants of orthotropic plates by modal analysis Rayleigh/Ritz techniques". J. Sound Vib., **124(2)**, 269-283(1988).

P.S. Frederiksen, "Single-layer plate theories applied to the flexural vibration of completely free thick laminates". J. Sound Vib., **186**,743-759(1995).

J. P. Kai, E. Viola, "Free vibration analysis of laminated composite plates". *Technical Report n°98* DISTART Department, University of Bologna, Bologna-Italy(2003),.

*Table 1. Comparison of dimensionless frequency parameter* $\bar{\omega}=\omega a^2\sqrt{\rho/\left(E_1h^2\right)}$ *obtained from Ritz models for a/b=1.5, a/h=30, for a three-layer angle-ply [θ, - θ, θ] plate.*

| | | Mode number | | | | | | | | | |
|---|---|---|---|---|---|---|---|---|---|---|---|
| θ(Angle) | Model | 1 | 2 | 3 | 4 | 5 | 6 | 7 | 8 | 9 | 10 |
| | HSDT-2 | 1.0346 | 1.4381 | 2.541 | 3.9318 | 4.994 | 6.2808 | 6.5892 | 7.5484 | 7.6908 | 8,6041 |
| 0 | FSDT-2 | 1.0347 | 1.4382 | 2.5411 | 3.9321 | 4.9941 | 6.2814 | 6.5895 | 7.5499 | 7.6892 | 8.6042 |
| | CLPT-1 | 1.0512 | 1.441 | 2.5856 | 3.9614 | 5.0911 | 6.4491 | 6.7821 | 7.7221 | 7.9116 | 8.8107 |
| | CLPT-2 | 1.0523 | 1.4443 | 2.5925 | 3.9814 | 5.1186 | 6.464 | 6.8008 | 7.7812 | 7.9527 | 8.8907 |
| | HSDT-2 | 1.208 | 1.4469 | 2.8021 | 3.9507 | 4.9449 | 6.2058 | 6.3032 | 7.4014 | 8.3205 | 8.8425 |
| | FSDT-2 | 1.2165 | 1.4491 | 2.8079 | 3.9617 | 5.0211 | 6.2187 | 6.3417 | 7.463 | 8.357 | 8.9679 |
| 15 | CLPT-1 | 1.2292 | 1.4502 | 2.8589 | 3.9854 | 5.0539 | 6.4062 | 6.5575 | 7.6362 | 8.6719 | 9.1539 |
| | CLPT-2 | 1.2306 | 1.4535 | 2.8666 | 4.0054 | 5.0751 | 6.4275 | 6.5779 | 7.6897 | 8.7256 | 9.2208 |
| | HSDT-2 | 1.4429 | 1.5334 | 3.2289 | 4.0321 | 4.6245 | 6.2247 | 6.6349 | 7.1396 | 9.4497 | 10.127 |
| | FSDT-2 | 1.4495 | 1.5343 | 3.2796 | 4.1363 | 4.6781 | 6.3983 | 6.7267 | 7.3881 | 9.8131 | 10.393 |
| 30 | CLPT-1 | 1.467 | 1.5449 | 3.3217 | 4.1369 | 4.7612 | 6.4439 | 6.9438 | 7.512 | 9.896 | 10.775 |
| | CLPT-2 | 1.4693 | 1.5482 | 3.331 | 4.1561 | 4.7727 | 6.4743 | 6.9697 | 7.5597 | 9.9616 | 10.86 |
| | HSDT-2 | 1.529 | 1.5941 | 3.4182 | 4.0898 | 4.3321 | 6.3997 | 6.8829 | 7.4294 | 9.3551 | 10.197 |
| | FSDT-2 | 1.5298 | 1.6003 | 3.4234 | 4.1619 | 4.4189 | 6.4423 | 6.8361 | 7.3664 | 9.8709 | 10.323 |
| 45 | CLPT-1 | 1.5614 | 1.6024 | 3.5322 | 4.2721 | 4.4618 | 6.637 | 7.3114 | 7.77 | 10.059 | 10.669 |
| | CLPT-2 | 1.5636 | 1.6065 | 3.5423 | 4.2897 | 4.47 | 6.6683 | 7.3599 | 7.8115 | 10.115 | 10.747 |

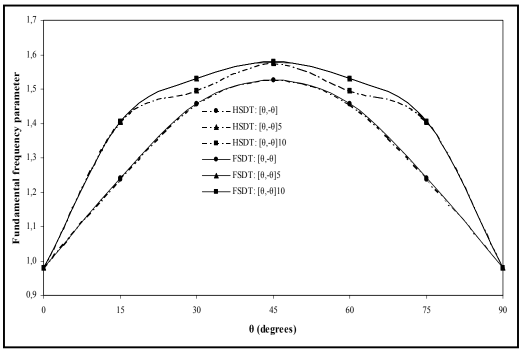


*Figure 1.*

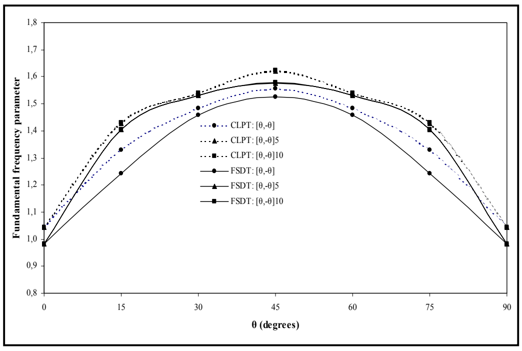


*Figure 2.*

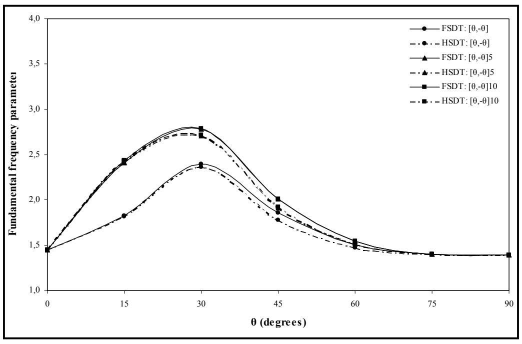


*Figure 3.*

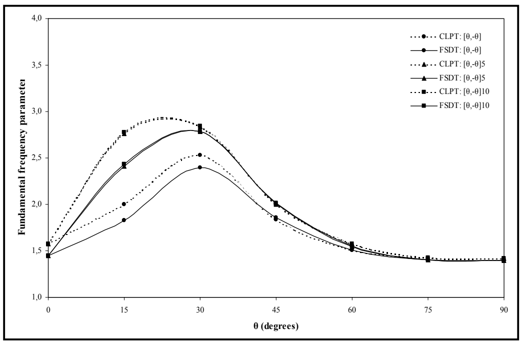


*Figure 4.*

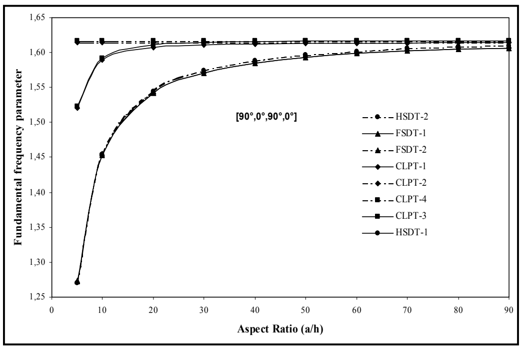


*Figure 5.*

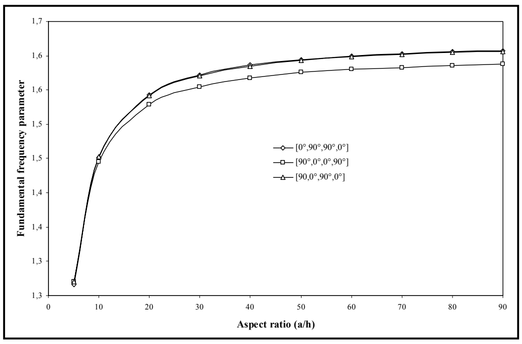


*Figure 6.*

*Figure 1- Representation of frequency parameter for HSDT and FSDT obtained from Ritz models for a/b=1 and a/h=10, for antisymetric angle-ply plate.*
*Figure 2- Representation of frequency parameter for FSDT and CLPT obtained from Ritz models for a/b=1 and a/h=10, for antisymetric angle-ply plate.*
*Figure 3- Representation of frequency parameter for HSDT and FSDT obtained from Ritz models for a/b=1.5 and a/h=10, for antisymetric angle-ply plate..*
*Figure 4- Representation of frequency parameter for FSDT and CLPT obtained from Ritz models for a/b=1.5 and a/h=10, for antisymetric angle-ply plate..*
*Figure 5- Effect of span depth ratio on the nondimensional fundamental frequency obtained from Ritz models for a/b=1.5, for a cross-ply rectangular plate.*
*Figure 6- Effect of span depth ratio on the nondimensional fundamental frequency for different cross-ply rectangular plates.*